

PROBING THE NUCLEAR STRUCTURE OF EXOTIC ^{33}Mg ISOTOPE

Haneen Waheed KADHIM

Al-Qasim Green University, Iraq

Rawaa Amer HAMEED

Al-Qasim Green University, Iraq

Mohammed Yahya HADI¹

Al-Qasim Green University, Iraq

Abstract

Research on the nuclear structure of exotic isotopes, such as ^{33}Mg , is an exciting and cutting-edge field of nuclear physics. Exotic isotopes are typically those that are far from the stable region of the nuclear chart and often exhibit unique properties that can help us better understand the fundamental forces and structure of atomic nuclei. In this paper the large-scale shell model calculations are performed within the model spaces SDPFMU, to study the positive- and negative-parity energy levels and electromagnetic transitions in the exotic ^{33}Mg isotope. Core-polarization effects on reduced transition probability are introduced through first order perturbation theory, which allows for higher energy configurations through excitations of nucleons from core orbits to that outside model space up to $9\hbar\omega$. The core-polarization effects have been improved the agreement of $B(E2)$ with their corresponding experimental data, and have ignorable effect on $B(M1)$.

Keywords: ^{33}Mg , The Nuclear Structure, Core-polarization.

 <http://dx.doi.org/10.47832/2717-8234.18.22>

¹  mohammedyahya81@gmail.com, <https://orcid.org/0000-0001-6549-0424>



Introduction

Investigation of characteristics of unstable atomic nuclei holds significant importance in the field of nuclear physics. Unstable nuclei, particularly those located near the drip line, exhibit extraordinary properties. One such property is the alteration of the well-established concept of magic numbers [1], [2] [3]. The conventional ordering of nuclear shells can undergo modifications as a consequence of residual interactions between nucleons. Consequently, certain shell gaps become less distinct, resulting in a change in the magic numbers. When a distinct shift in the magic numbers occurs within a specific region, that region is referred to as an "island of inversion" [4]. Within this region, nuclei demonstrate higher binding energies than expected, which can be attributed to collective phenomena such as rotation.

In this region, the presence of strong nuclear deformation was suggested based on low excitation energies and significant $B(E2)$ values observed for the first excited states of these nuclei [5-9]. More recently, Otsuka and collaborators highlighted the role of the nucleon-nucleon tensor interaction as a mechanism for the suppression of shell gaps [5]–[7]. Consequently, the $N=20$ magic number is believed to vanish in Ne, Na, and Mg isotopes.

there are proposed explanations for the strong nuclear deformation observed in the $N = 20 \sim 22$ region of Ne, Na, and Mg isotopes. One possible explanation is the emergence of intruder configurations involving higher-energy orbitals in the nuclear structure. In the traditional shell model, nucleons occupy specific energy levels or orbitals within the nucleus, forming magic numbers and well-defined shell closures. However, in the $N = 20 \sim 22$ region, the presence of intruder configurations from higher-energy orbitals can significantly influence the nuclear structure. The intruder configurations arise due to the interplay between the residual nucleon-nucleon interactions and the specific properties of the energy levels in this region. The $(sd)^{-2}(fp)^2$ intruder configuration, which involves excitations from the sd -shell to the fp -shell, has been proposed as a dominant configuration in the ground states of Ne, Na, and Mg isotopes.

The mixing of intruder configurations with the traditional shell model configurations leads to a breakdown of the usual magic numbers and results in strong nuclear deformation [8], [9]. The deformation manifests as changes in the shape of the nucleus, such as elongation or compression, which can be characterized by measured low excitation energies and large $B(E2)$ values for the first excited states in these isotopes. It is important to note that the understanding of the exact mechanisms behind the strong nuclear deformation in this region is an active area of research. Theoretical models, such as those incorporating the role of the nucleon-nucleon tensor interaction, are continuously being developed to provide a more comprehensive explanation for the observed phenomena.

We have performed the large scale shell model calculations for the ^{33}Mg within the model spaces sd_{pf} by using OXBASH code [10]. The inert cores of this model space is ^{16}O . The positive and negative parity states are calculated within $0, +1 \hbar\omega$ configurations of model

space which allowed excitations of one nucleon from 2s1d to 2p1f shells. In this calculate the adopted interactions was SDPFMU [11]. The calculation of reduced transition probability, core polarization effects are introduced such that 1p-1h configurations up to $9 \hbar\omega$ are taken into account. Also, OXBASH code is used to generate One-Body Density Matrix elements (OBDMs) which are important in the calculations of the reduced transition probabilities ($B(\omega J)$) between nuclear shell model states.

In the calculation of the electric transitions $B(EJ)$ and the magnetic transitions $B(MJ)$, core-polarization effects are introduced through microscopic theory that include excitations of nucleons from the core orbits into higher shells up to $9 \hbar\omega$ excitations outside model space, with $\hbar\omega = 45A^{-1/3} - 25A^{-2/3}$ [12]. The core orbits are 1s and 1p for sdpf model space. The results of $B(\omega J)$ that calculated within model space are denoted as MS, while that incorporated core-polarization effects are denoted as MS+CP.

This study aims to provide important new insights into nuclear structure around the N=20 island of inversion. While previous experiments and theories have offered significant glimpses, open questions still remain. By utilizing the extensive configuration interaction afforded through our large-scale shell model approach, we can generate a more comprehensive level scheme for ^{33}Mg and benchmark it against future measurements. This will help identify dominant components in the wave function and their role in driving deformation. Through systematically varying parameters like the excitation cutoff, we also seek to refine our understanding of core polarization effects. The degree to which higher-lying proton-neutron correlations impact observables tells us about emergent collective modes near the drip line. From our calculations, detailed spectroscopic predictions will be made available for the experiment work. This will enable new detection possibilities with reaccelerated isotope beams. Together theory and experiment form a mutually reinforcing partnership to unravel exotic single-particle phenomena in the most neutron-rich regimes.

1. THEORY

The reduced probability for the electromagnetic transition operator $O_{JT}^{\overline{\omega}}$ ($\overline{\omega} \equiv E$ or M for electric or magnetic operators) between the initial (i) and final (f) nuclear states of spin and isospin $\Gamma_i \equiv J_i T_i$ and $\Gamma_f \equiv J_f T_f$, respectively, is given by [13]:

$$B(\overline{\omega}J; i \rightarrow f) = \frac{1}{2J_i + 1} \left| \sum_{T=0,1} (-1)^{T_f - T_z} \begin{pmatrix} T_f & T & T_i \\ -T_z & 0 & T_z \end{pmatrix} (\Gamma_f ||| O_{JT}^{\overline{\omega}} ||| \Gamma_i) \right|^2 \quad (1)$$

where $\begin{pmatrix} \cdot & \cdot & \cdot \end{pmatrix}$ is the 3j-symbol, T is isospin. $T_{iz} = T_{fz} = T_z = (Z - N)/2$, and $\Gamma \equiv JT$. The T can take on two possible values: $T=0$ is called an isoscalar and $T=1$ is called an isovector. These values represent the different possible states that a particle can have under isospin symmetry. The concept of isospin is important because it allows physicists to describe the behavior of particles that have similar interactions but different masses or charges. By considering particles with different isospin values. The total isospin of a proton-neutron system can either be $T=1$ if the two isospins are aligned and $T=0$ if they are antialigned. The triple-bar matrix element is used to indicate the reduction in spin and isospin spaces. The reduced many-particle matrix elements are written in terms of reduced single-particle one, as [12]

$$(\Gamma_f ||| O_{JT}^{\overline{\omega}} ||| \Gamma_i) = \sum_{\alpha\beta} OBDM(\alpha, \beta, \Gamma_f, \Gamma_i, \Gamma) (\alpha ||| O_{JT}^{\overline{\omega}} ||| \beta) \quad (2)$$

where α and β denote the quantum numbers of single-particle states (including isospin), and the OBDM are defined by [12]

$$OBDM(\alpha, \beta, \Gamma_f, \Gamma_i, \Gamma) = \frac{\langle \Gamma_f ||| [a_{\alpha}^{\dagger} \times \tilde{a}_{\beta}]^{\Gamma} ||| \Gamma_i \rangle}{\sqrt{2\Gamma + 1}} \quad (3)$$

The inclusion of core-polarization effects on the one-body transition operator, through first-order perturbation theory, in the presence of the residual interaction V_{res} will separate the reduced single-particle matrix elements into three parts [12]

$$(\alpha ||| O_{JT}^{\overline{\omega}} ||| \beta) = \langle \alpha ||| O_{JT}^{\overline{\omega}} ||| \beta \rangle + \langle \alpha ||| O_{JT}^{\overline{\omega}} \frac{Q}{E_i - H_o} V_{res} ||| \beta \rangle + \langle \alpha ||| V_{res} \frac{Q}{E_f - H_o} O_{JT}^{\overline{\omega}} ||| \beta \rangle \quad (4)$$

The operator Q is the projection operator onto the space outside the model space. $E_{i,f}$ are the initial and final states energies. The first term is due to model space, while the second and third terms are due to core-polarization effects. The core-polarization terms can be evaluated in terms of the matrix elements of residual interaction and the transition operator

by introducing intermediate particle $|\alpha_1\rangle$ and hole $|\alpha_2\rangle$ states, and using some Racah algebra [12], [14]

$$\begin{aligned} & \sum_{\alpha_1 \alpha_2 \Gamma'} \frac{(-1)^{\beta + \alpha_2 + \Gamma'}}{e_\beta - e_\alpha - e_{\alpha_1} + e_{\alpha_2}} \\ & \times (2\Gamma' + 1) \begin{Bmatrix} \alpha & \beta & \Gamma \\ \alpha_2 & \alpha_1 & \Gamma' \end{Bmatrix} \\ & \times \sqrt{(1 + \delta_{\alpha_1 \alpha})(1 + \delta_{\alpha_2 \beta})} \\ & \times \langle \alpha \alpha_1 | V_{res} | \beta \alpha_2 \rangle \langle \alpha_2 || O_{\Gamma'}^{\overline{w}} || \alpha_1 \rangle \\ & + \text{terms with } \alpha_1 \text{ and } \alpha_2 \text{ exchanged with} \\ & \text{an overall minus sign,} \quad (5) \end{aligned}$$

The triple-bar single-particle matrix elements are written in terms of double-bar one, by [12]

$$\langle \alpha_2 || O_{\Gamma'}^{\overline{w}} || \alpha_1 \rangle = \sqrt{\frac{2T + 1}{2}} \sum_{t_z} P_T(t_z) \langle \alpha_2 || O_{j t_z}^{\overline{w}} || \alpha_1 \rangle \quad (6)$$

with

$$P_T(t_z) = \begin{cases} 1 & \text{for } T = 0, \\ (-1)^{1/2 - t_z} & \text{for } T = 1, \end{cases}$$

where T denotes the isospin, $t_z = 1/2$ for a proton and $-1/2$ for a neutron.

The single-particle energies in the denominator of eq.(5) are calculated by [12]

$$\begin{aligned} e_{n\ell j} &= \left(2n + \ell - \frac{1}{2}\right) \hbar\omega \\ &+ \begin{cases} -\frac{1}{2}(\ell + 1)\langle f(r) \rangle_{n\ell} & \text{for } j = \ell - 1/2 \\ \frac{1}{2}\ell \langle f(r) \rangle_{n\ell} & \text{for } j = \ell + 1/2 \end{cases} \\ & \text{with } \langle f(r) \rangle_{n\ell} \approx -20A^{-2/3} \\ & \text{and} \\ \hbar\omega &= 45A^{-1/3} - 25A^{-2/3} \quad (7) \end{aligned}$$

The reduced matrix elements of the electric and magnetic operators are given, respectively, by [12]

$$\begin{aligned} \langle a || O_J^E || b \rangle &= (-1)^{j_b + J - 1/2} \left\{ \frac{1 + (-1)^{\ell_a + \ell_b + J}}{2} \right\} \sqrt{\frac{(2J + 1)(2j_a + 1)(2j_b + 1)}{4\pi}} \\ & \times \begin{pmatrix} j_a & j_b & J \\ 1/2 & -1/2 & 0 \end{pmatrix} \langle n_a \ell_a | r^J | n_b \ell_b \rangle, \quad (8) \end{aligned}$$

and

$$\langle a || O_J^M || b \rangle = (-1)^{j_b+J-\frac{1}{2}} \left\{ \frac{1 - (-1)^{\ell_a+\ell_b+J}}{2} \right\} \sqrt{\frac{(2J+1)(2j_a+1)(2j_b+1)}{4\pi}} \times \begin{pmatrix} j_a & j_b & J \\ 1/2 & -1/2 & 0 \end{pmatrix} (J-\kappa) \left[g_\ell \left(1 + \frac{\kappa}{J+1} \right) - \frac{1}{2} g_s \right] \langle n_a \ell_a | r^{J-1} | n_b \ell_b \rangle, \quad (9)$$

with

$$\kappa = (-1)^{\ell_a+j_a+\frac{1}{2}} \left(j_a + \frac{1}{2} \right) + (-1)^{\ell_b+j_b+\frac{1}{2}} \left(j_b + \frac{1}{2} \right)$$

Where the notation $\langle n_a \ell_a | r^J | n_b \ell_b \rangle$ represents the matrix element between two single-particle states, characterized by their quantum numbers $(n_a \ell_a)$ and $(n_b \ell_b)$, and refers to the radial part of the final and initial wave function respectively. the g-factors are $g_\ell^p = 1, g_s^p = 5.5857, g_\ell^n = 0, g_s^n = -3.8263$ for the proton and the neutron respectively, and the radial integral involving harmonic oscillator radial wave functions $R_{n\ell}(r)$ are defined as

$$\langle n_a \ell_a | r^\lambda | n_b \ell_b \rangle = \int_0^\infty R_{n_a \ell_a}(r) r^\lambda R_{n_b \ell_b}(r) r^2 dr \quad (10)$$

2. Results and Discussion

The utilized residual interaction is referred to as the Modified Surface Delta Interaction (MSDI). Within the MSDI model, the strength parameter denotes the intensity of the close-range delta potential, which characterizes the robust interaction between nucleons when they are in close proximity within the atomic nucleus. This parameter is assigned values of approximately $A_0 \approx A_1 \approx B \approx \frac{25}{A} \text{ (MeV)}$, while C is approximately 0. Here, A represents the atomic mass [12], [15].

Both the experimental and the theoretical level schemes of the ^{33}Mg nucleus are depicted in Figure 1. The calculations for the sd-pf shell model are carried out by the interaction of 17 nucleons, which consist of (4 protons + 13 neutrons). The overall state of this isotope is characterized by negative energy levels, primarily because there is a lone nucleon residing within the pf shell, while the positive parity states resulted from the sharing of one nucleon's jump from the sd to the pf orbital, as we limited the transition to $0, +1 \hbar\omega$ [16]. It is important to mention that the levels generated by the sd-pf model space yielded the most

favorable outcome compared to other calculations and exhibited the closest resemblance to the experimental values.

In a comprehensive analysis, it is observed that the calculated excitation energy levels within the sd₂pf model exhibit remarkable agreement with the validated experimental values [17]. It is noteworthy that the energy level at 0.705 MeV is associated with experimental uncertainty, as multiple values for J have been reported as $(1/2+, 3/2+, 5/2+)$. Among these values, it is anticipated that one of them corresponds to the true value of J . Through our computational analysis utilizing effective interactions, specifically SDPFMU, we have obtained a $J = (5/2 +)$ value at an energy level of $E_x=0.654$ MeV. The convergence of these results lends support to the possibility of considering this value as the official $J = (5/2 +)$ level.

Figure 1 provides a lucid depiction of the projected quantity of levels attained through the utilization of shell model calculations. The notable achievement in effectively ascertaining the ground level for this specific isotope, which exhibits a remarkable concordance with experimental measurements, engenders a plausible opportunity to harness the outputs of these calculations in the appraisal of excited states. These computed values manifest considerable promise as dependable standards in forthcoming scholarly undertakings about this isotope.

This study investigates the reduced transition probability $B(\omega J)$ within the model space (MS) and explores the impact of Core-polarization effects (CP), denoted as (MS+CP). The influence of CP on the reduced transition probability is examined using first-order perturbation theory.

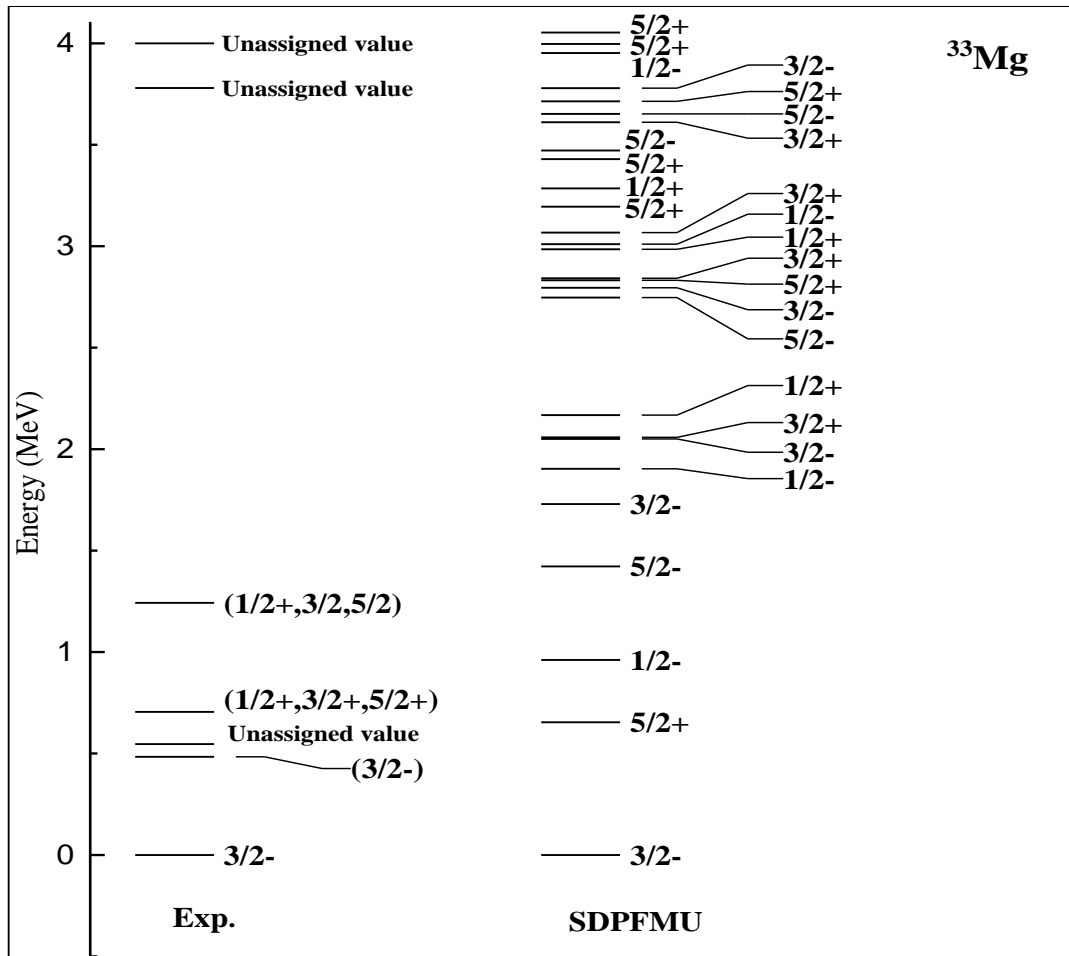


Figure 1. Represents the comparison of the energy levels of the ^{33}Mg isotopes computed in the model space (*sdpf*) with the experimental values (Exp.) [17].

According to this theory, nucleons can be excited from core orbits to orbits outside of the model space, up to $n\hbar\omega$. In this work, we consider up to $9\hbar\omega$, thereby accommodating higher energy configurations.

Table 1 presents the computed values for the reduced electric transition $B(EJ)$ and reduced magnetic transition $B(MJ)$ of interest. The $B(E2)$ values for the isotope ^{33}Mg is derived from the SDPFMU interactions, expressed in Weisskopf units (W.U.) [18] [19]. Although experimental data for comparison is lacking, the obtained results are intriguing. Notably, the result agrees with the opinion of W. Zhang et al. [20], who indicated in their research in atomic nuclei with even numbers of neutrons and protons, a decrease in the energy of the initial excited ($2+$) state is followed by an increase in the ($2_1^+ \rightarrow 0_{\text{gs}}^+$) probability of the $B(E2)$. Overall, modified values between the MS and MS+CP calculations are particularly evident in the $B(E2)$ values, while for the $B(M1)$ transitions show no effect. Core-polarization effects may have a smaller effect on $B(M1)$ transitions compared to $B(E2)$ transitions due to the mechanism involved [21]. $B(M1)$ transitions primarily involve the spin-flip of individual nucleons, and the magnetic moment associated with the nucleon's intrinsic spin dominates the transition. This aspect is less directly influenced by core-polarization effects. The core-polarization-induced modifications to the spin distribution or magnetic moments are generally smaller in magnitude compared to the effects on quadrupole deformation and collective motion in $B(E2)$ transitions. Furthermore, $B(E2)$ transitions are more likely to exhibit collective behavior, with strong correlations between the core and valence nucleons. Core-polarization effects enhance this coupling, resulting in larger modifications to the transition probabilities. In contrast, $B(M1)$ transitions typically involve single-particle properties and are less sensitive to collective effects, leading to a reduced effect of core polarization. While core-polarization effects may have a smaller impact on $B(M1)$ transitions, it's important to note that they can still play a role, especially in specific cases where core-polarization-induced modifications to the spin distribution or magnetic moments are significant. The magnitude of these effects depends on the specific nuclear system, the energy of the excited states, and the strength of the core-valence nucleon coupling.

Table 1. prediction values of $B(\omega J)$ for ^{33}Mg in Weisskopf units (W.U.) [19].

$2J_{ni}^{\pi} \rightarrow 2J_{nf}^{\pi}$	Exp.	sdpf		$B(\omega L)$
		MS	MS+CP	
$1_1^- \rightarrow 3_1^-$		3.705	8.252	E2
$1_2^- \rightarrow 3_1^-$		0.584	0.688	E2
$3_2^- \rightarrow 3_1^-$		0.352	0.387	E2
$3_3^- \rightarrow 3_1^-$		1.467	1.607	E2
$5_1^- \rightarrow 3_1^-$		1.473	1.701	E2
$5_2^- \rightarrow 3_1^-$		0.121	0.152	E2
$5_3^- \rightarrow 3_1^-$		0.056	0.054	E2
$5_1^- \rightarrow 1_1^-$		0.404	0.572	E2
$5_2^- \rightarrow 1_1^-$		1.713	2.033	E2
$5_3^- \rightarrow 1_1^-$		0.366	0.454	E2
$3_2^- \rightarrow 1_1^-$		1.091	1.095	E2
$3_3^- \rightarrow 1_1^-$		0.015	0.033	E2
$1_1^- \rightarrow 3_1^-$		1.134	1.134	M1
$1_2^- \rightarrow 3_1^-$		0.165	0.165	M1
$3_2^- \rightarrow 3_1^-$		0.138	0.138	M1
$3_3^- \rightarrow 3_1^-$		0.009	0.009	M1

3. CONCLUSION

The shell model with configuration interaction is applied to the ^{33}Mg isotope to generate positive- and negative-parity states and calculate the reduced transition probabilities between them. To accomplish this task, a single model space, namely the sd₂p₂f space, is utilized. The positive- and negative-parity states in the exotic ^{33}Mg isotopes are accurately reproduced by calculations performed within the SDPFMU interaction. In our work, instead of relying on free parameters, we employ microscopic theory without the use of any free parameter to calculate $B(EL)$ and $B(ML)$ for the model-dependent calculations of reduced transition probabilities. Core-polarization effects are taken into account, considering intermediate particle-hole excitations in the presence of residual interaction. The inclusion of microscopic core-polarization effects, in conjunction with the presence of $MSDI$ as the residual interaction, enhances the results of $B(E2)$. However, no effect of core polarization on $B(M1)$ is observed.

References

- [1] M. G. Mayer, "On Closed Shells in Nuclei. II," *Phys. Rev.*, vol. 75, no. 12, pp. 1969–1970, Jun. 1949.
- [2] O. Haxel, J. H. D. Jensen, and H. E. Suess, "On the 'Magic Numbers' in Nuclear Structure," *Phys. Rev.*, vol. 75, no. 11, pp. 1766–1766, Jun. 1949.
- [3] O. Sorlin and M.-G. Porquet, "Nuclear magic numbers: New features far from stability," *Prog. Part. Nucl. Phys.*, vol. 61, no. 2, pp. 602–673, Oct. 2008.
- [4] E. K. Warburton, J. A. Becker, and B. A. Brown, "Mass systematics for $A=29-44$ nuclei: The deformed $A\sim 32$ region," *Phys. Rev. C*, vol. 41, no. 3, p. 1147, 1990.
- [5] N. Tsunoda *et al.*, "The impact of nuclear shape on the emergence of the neutron dripline," *Nature*, vol. 587, no. 7832, pp. 66–71, 2020.
- [6] H. J. Ong, "Understanding Effect of Tensor Interactions on Structure of Light Atomic Nuclei," *Few-Body Syst.*, vol. 62, no. 4, p. 86, 2021.
- [7] T. Otsuka and Y. Tsunoda, "The role of shell evolution in shape coexistence," *J. Phys. G Nucl. Part. Phys.*, vol. 43, no. 2, p. 24009, 2016.
- [8] N. Kitamura, "Nuclear structure at the border of the island of inversion: in-beam γ -ray spectroscopy of ^{30}Mg ." 東京大学, 2020.
- [9] T. Otsuka, A. Gade, O. Sorlin, T. Suzuki, and Y. Utsuno, "Evolution of shell structure in exotic nuclei," *Rev. Mod. Phys.*, vol. 92, no. 1, p. 15002, 2020.
- [10] B. A. Brown *et al.*, "Oxbash for windows PC," *MSU-NSCL Rep.*, vol. 1289, 2004.
- [11] Y. Utsuno, T. Otsuka, B. A. Brown, M. Honma, T. Mizusaki, and N. Shimizu, "Shape transitions in exotic Si and S isotopes and tensor-force-driven Jahn-Teller effect," *Phys. Rev. C*, vol. 86, no. 5, pp. 1–6, 2012.
- [12] P. J. Brussaard and P. W. M. Glaudemans, *Shell-model applications in nuclear spectroscopy*. Elsevier, 1977.
- [13] T. W. Donnelly and I. Sick, "Elastic magnetic electron scattering from nuclei," *Rev. Mod. Phys.*, vol. 56, no. 3, pp. 461–566, Jul. 1984.
- [14] A. A. Al-Sa'ad and A. A. Abbass, "Core-polarization effects on the isovector magnetic dipole transitions in ^{24}Mg ," *Chinese J. Phys.*, vol. 50, no. 5, pp. 768–775, 2012.
- [15] A. Heusler and P. von Brentano, "Mass dependence of the surface δ -interaction strength for two-particle (two-hole) multiplets," *Eur. Phys. J. A*, vol. 38, no. 1, pp. 9–16, Oct. 2008.
- [16] M. Bouhelal, F. Haas, E. Caurier, F. Nowacki, and A. Bouldjedri, "A PSDPF interaction to describe the $1\hbar\omega$ intruder states in sd shell nuclei," *Nucl. Phys. A*, vol. 864, no. 1, pp. 113–127, 2011.
- [17] National Nuclear Data Center, "Evaluated and Compiled Nuclear Structure Data," *International Network of Nuclear Structure and Decay Data Evaluators*. [Online]. Available: <https://www.nndc.bnl.gov/ensdf/>.

- [18] S. S. M. Wong, *Introductory nuclear physics*, 2nd ed. Weinheim SE - XII, 460 p. : graf. ; 24 cm: Wiley-VCH Weinheim, 2004.
- [19] B. A. Brown, *Lecture Notes in Nuclear Structure Physics*. Michigan State University, 2011.
- [20] W. Zhang *et al.*, "Lifetime measurements of excited states in $^{169,171,173}\text{Os}$: Persistence of anomalous B(E2) ratios in transitional rare earth nuclei in the presence of a decoupled $i_{13/2}$ valence neutron," *Phys. Lett. B*, vol. 820, p. 136527, Sep. 2021.
- [21] J. Chen *et al.*, "Probing the quadrupole transition strength of C 15 via deuteron inelastic scattering," *Phys. Rev. C*, vol. 106, no. 6, p. 64312, 2022.